POLITECNICO DI TORINO
Repository ISTITUZIONALE

Module Level Electronic Circuit based PV array for Identification and Reconfiguration of Bypass Modules

(Article begins on next page)

26 December 2024

Module Level Electronic Circuit based PV array for Identification and Reconfiguration of Bypass Modules

Ali F Murtaza[1,2], *Member IEEE*, Hadeed Ahmed Sher[3], *Senior Member IEEE,* Kamal Al-Haddad[4], *Fellow IEEE*, Filippo Spertino[5]

[1]Corresponding Author: Faculty of Engineering, University of Central Punjab, 1-Khyaban-e-Jinnah Road, Lahore, Pakistan. Email: ali.faisal@ucp.edu.pk
[2]Faculty of Engineering, University of Central Punjab, 1-Khyaban-e-Jinnah Road, Lahore, Pakistan.
[3]Faculty of Electrical Engineering, Ghulam Ishaq Khan Institute of Engineering Sciences and Technology, Topi, Pakistan
[4]École de Technologie Supérieure (ÉTS), University of Quebec, Montreal, QC, Canada
[5]Department of Energy, Politecnico di Toino, Italy

Abstract— **In this paper, a novel electronic circuit based on optocoupler is designed for each module of photovoltaic (PV) array to deal with partial shading conditions. The proposed circuit not only provides electronic monitoring at the module level but also ensures the reconfiguration of bypass modules. The control framework of the proposed scheme works in two steps. In *Step-1*, the PV array is connected in series-parallel (SP) configuration and the power-voltage (P-V) curve is traced to search the global maximum (GM). In *Step-2*, bypass modules are separated from PV array through their respective electronic circuits in a decentralized control manner, and the power of bypass modules is stored in the battery. The proposed electronic circuit provides a low cost solution as it is free from expensive sensing and complex switching network. Moreover, the control operation of proposed scheme is simple. The proposed scheme is verified through computer-aided simulations and a hardware prototype of 170 W. The comparative study indicates that the proposed scheme yields more energy than past proposed solutions.**

Index Terms—**Reconfigurable PV array, Dynamic reconfiguration methods, MPPT, Partial shading effects.**

I. INTRODUCTION

Photovoltaic (PV) modules receive irradiance levels of different magnitudes when the PV array is under the influence of partial shading. This situation results in current imbalance from module to module level with-in a string and from string to string level with-in a PV array [1-2]. As a result, the current-voltage (I-V) curve of PV array transforms into a complex waveform containing multiple local maxima (LMs). Among them, the maximum power bearer is called the global maximum (GM) [3-4]. Fig. 1 depicts the power-voltage (P-V) curve (red line) of PV array when it is under the influence of partial shading [4-6]. Under such operating conditions, even if the GM is achieved through a sophisticated MPPT algorithm, the useful power of bypass modules is wasted [7]. Note that closer the GM to the short circuit current, more are the shaded modules, and hence more power loss. If the energy of bypass modules is recovered, the P-V curve covers up the partial shading or mismatch loss and only suffers from the shading losses as cleared from the blue line curve in Fig. 1.

In the recent past, scientists proposed the concept of dynamic PV array; which reconfigures the electrical connections of PV modules with-in a PV array [1-3, 6-7]. This concept comes in the following three ways:
1) PV array is rearranged for irradiance equalization at the string level i.e., the strings are arranged to have equal irradiance levels [2-3,7].
2) PV modules are rearranged in different interconnection schemes such as tied-cross-tied (TCT), honey-comb (HC), series-parallel (SP), etc., and amongst them, the scheme which delivers the maximum power is selected [5-6,8-9].
3) The optimization methods are used to find a better interconnection scheme [1,9-15].

A particle swarm optimization (PSO) method is adopted in [1] to rearrange the array. This method yields better energy than TCT, SuDoku, and genetic algorithm (GA). However, the involvement of several inherited coefficients and irradiance patterns formulated through numerous iterations make this method expensive in the context of fast processing device and RAM size. For instance, 81 irradiance values are computed in each of 500 iterations while working with an array of 9 x 9. Moreover, in each iteration, row-wise power and current difference need to be calculated for updating the local best and global best points. The number of switches and undesired configurations is successfully reduced in [9], but with a complex objective function of PSO. The transformation of PSO towards PV system is not straight forward as innate parameters of PSO such as population size, acceleration constants, inertia weight constants, and objective function are difficult to tune and may vary with different array sizes. The power comparison scheme is successfully applied to SP and TCT configurations in
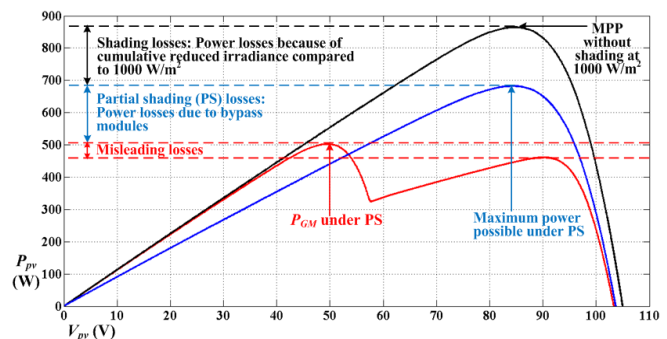

Fig. 1 An overview of I-V curves depicting the power difference between shading loss and mismatch loss

[3]. However, the principle operation of this method requires numerous current sensors. Similarly, [4] has provided optimal array reconfiguration technique based on current sensing for each module and voltage sensing for each row. The placement, positioning, and data acquisition of sensors create several challenges in the practical implementation of this method.

A continued swapping of PV modules through the greedy algorithm is the hallmark philosophy of [10], where a PV array is divided into the fixed and reconfigurable part. The number of switches required for optimal reconfiguration is equal to the number of reconfigurable modules. Consequently, this method requires numerous switches/relays, due to which following constraints occur: 1) switching losses and delays, 2) gate driving circuits, and 3) additional wiring. It also implies that this method is not scalable to large PV arrays.

In [11], the exhaustive computations of reconfiguration algorithm are filtered in case of repeated shading patterns. Nevertheless, the computation cost of the algorithm is still high during distinct shading patterns. An efficient optimization mechanism is proposed in [12], however; extensive matrices and stochastic procedures are the demands of this method. In [13], the method predicts the interconnection of modules in TCT configuration and provides multiple possible solutions. In hindsight, this method is technically a complex solution.

A real cloud pattern based adaptive reconfiguration technique is presented in [14]. The technique is better in terms of simplicity and scalability; however, it requires the data of incident irradiance profile. Moreover, smaller irradiation thresholds lead to an increased number of switching operations, which in turn results in increased switching losses. In [16], line losses are reduced in puzzled PV array configuration at the expense of sizable computations of sub-matrices.

Concerning the financial feasibility of reconfigurable PV array, a cost-analysis based study is conducted in [17]. This study concluded that reconfigurable PV array is economically profitable in locations where the phenomenon of partial shading is frequent and occurs daily during high energy generation periods. Recently, the reconfiguration scheme based on maximum and minimum (M^2) algorithm is used to identify the global maximum with a reduced number of electrical interconnections [18]. Nevertheless, the practical implementation of this method requires numerous relay switches, the management of which is not simple and straight forward. In [19], the PV array is first arranged in conventional series-parallel architecture, and the P-V curve is traced. Thereafter, each string is divided into two equal segments, and all half strings are connected in parallel to form the PV array. Once again, the P-V curve is scanned, and whichever configuration delivers the maximum power is selected. However, the twice tracings of P-V curve for every new shading condition incur the power loss in the PV system.

The main focus of techniques [20-21] is to reduce the mismatching loss by dispersing the partial shading effect across the PV array without changing the electrical connections. The method presented in [20] worked with TCT configured array and applied the improved SuDoKu algorithm for the estimation of optimum configuration. While method [21] utilized the chaotic baker map (CBM) algorithm to evaluate the best configuration. Similarly, the estimation of the irradiance value

of each module and their sorting is executed to distribute the shadow impact in [22]. These methods [20-22] are successful in reducing the partial shading effects. However, in their fundamental operation, not only the meta-heuristic algorithm is required for sorting, but also the physical movement of PV modules makes these methods difficult to implement practically, especially for large PV arrays.

From the aforementioned literature survey, it can be deduced that implementing a dynamic relocating algorithm for PV modules is not a trivial approach. Following procedures are adopted in one form or another [1,6, 9-10,15-16]:

1) Irradiance profile of each module: The extortionate irradiance sensor and complex mathematical models are required to estimate the irradiance of each module [8,11-12,15]. On the other hand, some methods interface the analog sensors with each module for the same purpose [1-2,6].

2) Searching and sorting algorithm: For the searching and sorting of modules with the same irradiance levels, the meta-heuristics algorithms are installed to optimize the reconfiguration of PV array [1-2,4,17].

3) Switching matrix: A network of switches is generated, which is further controller by a central hub. The number of switches for each module is always greater than 4 and sometimes more than 8 switches per module are required [1-2,6,11-12,15].

4) Scanning of P-V curve: Before setting the PV array at a particular interconnection, the P-V curve is traced multiple times for different configurations to find out the optimal configuration.

5) Scalability: The majority of the methods have scalability issues as their searching-sorting algorithms and irradiance estimation models are developed keeping in view the specific size of array.

In an attempt to rectify the aforementioned drawbacks, this paper introduces a sensor-less hardware scheme with simplified control, which inculcates the dynamic allocation of PV modules in a series-parallel (SP) array. In the proposed scheme, initially, all the modules are engaged in a normal SP manner and GM is tracked after scanning the P-V curve. Thereafter, the bypass modules are automatically separated from the PV array through optical devices. The energy of separated modules is then stored in a battery, which can be further transmitted to on-grid/off-grid applications through a dedicated dc-dc converter. In summary, the following contributions are made by the proposed hardware scheme:

♦ For the first time, the application of the optical device (known as optocoupler) is used for the dynamic allocation of PV modules, which makes the sensor-less control of PV array.

♦ The opto-IC based electronic circuit is connected to each module, where the circuit observes its specific module and relocates the module in a decentralized manner.

♦ The proposed circuit is simple, inexpensive, low power consumption, and a single IC-based solution.

♦ The design of a single electronic circuit is independent of the PV array size and power. Thus, it has no scalability issue and can be used to any array size.

II. ELECTRONIC CIRCUIT OF OPTOCOUPLER IC INTERFACING WITH PV MODULE

Optocoupler integrated circuit (opto-IC) is an electronic component that transfers an electrical signal between two isolated circuits by utilizing light as a medium [23]. From the manufacturing point of view, this chip is generally comprised of a light emitting diode (LED) at the input and a phototransistor at the output, which are coupled through an optical transfer medium behaving as an insulator in a single opaque package [23].

The interfacing of PV array using an optocoupler is presented in Fig 2. The electronic circuit consists of an optocoupler IC (opto-IC) of model k817p [24], and two resistors. The input of opto-IC is connected with the bypass diode of PV module through a forward resistance (R_F) and the output is connected to the biasing power supply (V_{CC}) through collector resistance (R_C). Note that the LED-photoemitter of the opto-IC along with the R_F comes in antiparallel connection with the bypass diode. This means that the opto-IC can be used to distinguish between the conducting and blocking states of the bypass diode i.e., the active or bypass status of PV module.

In Fig. 2(a), the PV module can carry the common string current (I_{string}), whereas the associated bypass diode remains in a reverse-biased condition. Under this case, the output (collector voltage) of the opto-IC shall remain in 'LOW' state as a photo-transistor operates in saturation mode. Contrary to that in Fig. 2(b), the PV module is represented to have partial shading, therefore, it cannot support the I_{String} and its bypass diode is active. Consequently, the input voltage of opto-IC remains 'LOW', thus making the output voltage 'HIGH' as a photo-transistor operates in cut-off mode.

In the proposed circuit, the opto-IC of model k817p [24] has the typical forward voltage (V_F) of 1 V. The forward current (I_F) of 100 µA is chosen. Assuming the minimum PV module's voltage (V_{Mod_Min}) as 1.5 V, the value of R_F is calculated as follows:

$$R_F = \frac{V_{Mod\_Min} - V_F}{I_F} = \frac{1.5 - 1.0}{100\ \mu} = 5\ k\Omega \qquad (1)$$
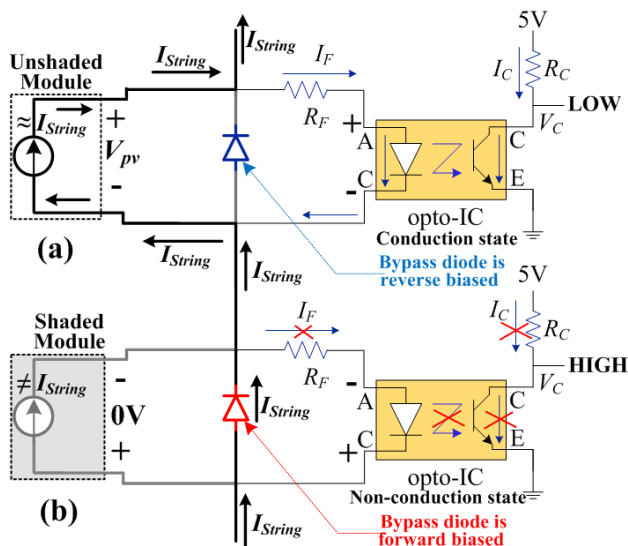

(a)

(b)

Fig. 2 Basic architecture of optocoupler IC interfacing with PV module & bypass diode: (a) active module, and (b) bypass module

Note that the choice of 1.5 V for V_{Mod_Min} is a sane estimation as the probability of a GM below 1.5 V is almost zero. Following this assumption, the optocoupler IC must turn ON for a voltage range of 1.5 V - V_{oc} of the PV module.

On similar grounds, using (2) the design of output collector resistance (R_C) is expressed in (3).

$$I_C = \underbrace{CTR \times I_F}_{\text{Opto-IC}} \equiv \underbrace{\beta \times I_B}_{\text{Transistor}} \qquad (2)$$

Where CTR is the current transfer ratio of opto-IC. It is similar to β or hfe gain of a bipolar junction transistor. CTR is a unitless quantity and is represented in percentage unit. The value of CTR is specified in the manufacturer's datasheet [24]. Under normal operating conditions, the CTR is 100% at $I_F = 10$ mA. In our case, I_F equals to 100 µA is selected because of the reason that opto-IC should not produce any loading effect on PV module i.e., a small current is drawn from the PV module. At this I_F, the safe estimation of CTR is 10% [24], which always drives the opto-IC in saturation mode. The scaling factor between I_F and CTR can be estimated from opto-IC datasheet. V_{CC} is the supply voltage that is set at 5 V. V_{CE_Sat} is the saturation voltage between collector and emitter, the typical value of which is 0.3 V [24].

$$R_C = \frac{V_{CC} - V_{CE\_Sat}}{I_C} = \frac{V_{CC} - V_{CE\_Sat}}{CTR \times I_F} \qquad (3)$$
$$= \frac{5 - 0.3}{0.1 \times 100\ \mu} = 470\ k\Omega$$

For the installation of opto-IC, following design constraints are discussed:

1) *Opto-IC design for different PV modules:* With regard to PV array, the parameters of opto-IC depend upon its input port condition, output port condition, and optical properties. In the proposed design, the opto-IC of model k817p is used, whose optical properties (CTR etc.) are estimated with a well-conservative manner to operate the device in saturation mode. Now, the output port of opto-IC is connected with the biasing supply of 5 V through a collector resistance R_C. Note that, these output parameters are independent of the PV array characteristics.

At the input port of opto-IC, the value of forward resistance R_F is selected based on the minimum voltage of the PV module ($V_{mod\_min} = 1.5$), which is valid for all PV modules. However, the maximum voltage rating (V_{Mod_Max}) of different modules increases the forward current (I_F), which, in turn, may violate the maximum current rating of the opto-IC. Using V_{Mod_Max}, the maximum value of I_F can be computed from (1).

For instance, the opto-IC of model k817p can withstand the maximum I_F of 60 mA [24]. In this sense, the proposed circuit can work appropriately for PV modules having voltage ratings well over 100 V. In case, an opto-IC of a different model is selected, the designer can follow the footprints of proposed opto-IC designing.

2) *Reverse voltage:* The reverse voltage handling capability of k817p is -6 V [24], the opto-IC should be able to withstand the forward voltage drop of the bypass diode (usually 0.7 V).

3) *Power consumption:* The power consumed in the sensing

of each module should be a fraction of the MPP. For instance, if the PV module operates at MPP with V_{mpp} = 16 V, I_{mpp} = 6 A and P_{mpp} = 96 W, (1) indicates that the proposed circuit eats up 3 mA of forward current (I_F) in sensing with R_F = 5 kΩ. Consequently, power comes out as 16 x 3 m = 48 mW, which is 0.05% of P_{mpp}.

4) *Galvanic isolation:* The insulation resistance should be high enough, such that it can withstand voltage spikes. The chosen opto-IC in the proposed system has insulation resistance of 10^{12} Ω and can handle a surge of 6 kV [24]. Due to this capability, the shielding devices such as zener diodes, opamps, etc., are not required, and therefore, it is a one-package solution.

5) *Cost, spacing, and installation point:* The procurement of single opto-IC is almost negligible (nearly 0.3 $), and merely 2.54 mm of space is required to install this electronic chip. The opto-IC can be installed near the junction box of PV module, where electronic components such as bypass diodes are pre-installed by the module manufacturer.

6) *Temperature withstanding capacity:* Likewise bypass diodes, opto-IC is an electronic component that can also work on high operating temperatures. Also, the natural air evolution between the ground and below side of the PV module helps in bringing down the operating temperature of opto-IC.

The precise ambient temperature range ($T_{amb\_Min} – T_{amb\_Max}$) of opto-IC can be studied from the manufacturer's datasheet to ensure the durability and safe operation of the IC. However, the maximum temperature of the installed location should be 20ºC less than T_{amb_Max} of opto-IC. Here, 20ºC is selected as a safety margin. For instance, the opto-IC of model k817p can operate between the temperature range of -40ºC to 100ºC [24]. However, with caution of 20ºC, this device can easily work between -40ºC to 80ºC. In most parts of the world, it is difficult to cross the ambient temperature of 80ºC. Nevertheless, the opto-IC with high withstanding temperature can be selected for those locations where temperature may reach higher levels.

A. Proposed functional circuit for a sensor-less PV system

Fig. 3 shows the proposed practical circuit for each module, in which two electromechanical relay switches (S_1 and S_2) of type single pole double throw (SPDT) are introduced. Under normal operation, PV module is interfaced with normal contact of relays such that it gets connected with bypass diode and opto-IC. Whenever the coils of relays are energized, they change their switch positions to active contact. Consequently, PV module becomes separated from PV array and starts storing its power in battery. The control sequence of switches is explained
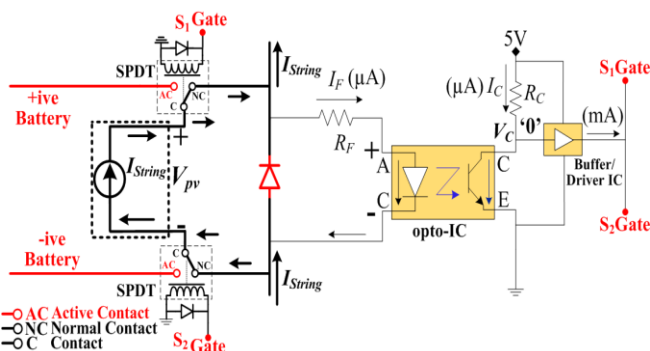
in the next section.

As already established that at any operating voltage (V_{pv}), the active or bypass status of a module can be identified through the collector voltage (V_C) of its opto-IC. The state of the V_C signal is utilized for automatic and decentralized control of S_1 and S_2 as described here:

♦ When S_1 and S_2 are in OFF-state due to V_C being 'LOW', it means that the PV module is operating at some value of $V_{pv,}$ and bypass diode is in reverse bias condition. Therefore, S_2 provides the path for I_{String} via its normal contact to flow through the PV module, and then I_{String} rejoins the string after passing through normal contact of S_1.

♦ When S_1 and S_2 are turned ON due to V_C being 'HIGH', it means that PV array is not operating at any V_{pv} and is bypassed. During this scenario, the active status of opto-IC energizes the coils of S1 and S2. These switches, in turn, change their respective switch positions to active contact. Consequently, the PV module is disengaged from PV array and is relocated through active contacts of S1 and S2, while bypass diode provides the path for I_{String}. In this way, the power of the shaded module can be used or stored.

The proposed practical circuit is quite feasible in terms of both power consumption and cost. The role of relay and unity buffer can be practically realized through relay model Finder 34.51 (rated current 6 A), and operational amplifier IC LM358, respectively. The power consumption of both devices is in milli-Watts.

The aforementioned discussion highlights that the design of the unit electronic circuit is based on opto-IC, which observes its specific module and relocates the module in a decentralized manner. In this sense, the design of the unit electronic circuit remains the same for any size of PV array including switches, components, power requirements, and other aspects. Besides, the decentralized control of each module by its respective electronic circuit does not increase the requirements of a centralized embedded system for large PV arrays in the context of numerous analog-to-digital channels, multiple switching signals, intense programming subroutines, and algorithm's complexity.

III. COMPLETE OPERATION OF PROPOSED ARCHITECTURE WITH CO-MPPT CONTROL

A layout of the proposed architecture is shown in Fig. 4(a) with one PV string. A separate battery (V_B) is connected to store the power of bypass modules. Fig. 4(a) reveals that each module forms a series connection with other modules through normal contacts of its respective switches S_1 and S_2. Under normal conditions, the power of modules is transferred to load. On the other hand, each module forms a parallel connection with the battery and other modules through active contacts of its respective switches S_1 and S_2. Under partial shading conditions, the shaded modules are bypassed and their power is stored in the battery. Note that different irradiance levels on PV modules produce a negligible impact in parallel connections since the condition of common series current does not exist. The voltage of the battery (V_B) can be set up at the V_{mpp} of module, the value of which can be determined from the manufacturer's datasheet.

For comprehensive understanding of sequence of switches,

Fig. 3 A practical circuit of optocoupler IC for each module

consider the following two-step flow of control method:

***Step-1*: a)** Disable all optocoupler ICs by cutting off the power at collector end, **b)** Trace P-V curve through a parallel capacitor to search the global maximum (GM), **c)** Set PV array at GM through modulating the duty cycle (*D*) of boost converter, *Goto Step-2.*

Step-2*: a)** Enable all optocoupler ICs by providing the power at collector end, **b)** Is present power close to GM/MPP: **Yes:** Stay Here*,* **No:** Goto ***Step-1.

The aforementioned steps indicate that in *Step-1*, the control unit disables all the opto-ICs by cutting-off the common power supply (V_{CC}). This mechanism is observed in Fig. 4(a), where each opto-IC receives Gnd signal at their power rail and gives low output at the V_c irrespective of its photo-emitter diode being forward biased or reverse biased. Consequently, the switches S_1 and S_2 of each module are deactivated, and all PV modules are organized in SP configuration through normal contacts of relays. Then, the P-V curve is traced through a parallel capacitor and GM is searched [25]. Once GM is tracked through modulation of D $(= D_{mpp})$ of the boost converter as shown in Fig. 4(b), the proposed method enters into *Step-2*.

In *Step-2*, the control unit simply switches ON the power rail of opto-ICs and initializes the new cycle if the present power is not in close proximity of the stored power of GM/MPP. Consider that when GM is obtained, the middle module (M_2) of the string is bypassed as shown in Fig. 4(b). As soon as power is supplied to opto-ICs in *Step-2*, V_C of opto-IC of the only middle module (M_2) becomes settled at 5 V i.e., '1', as shown in Fig. 4(c). Consequently, the coils of switches S_1 and S_2 of only module M_2 are energized automatically, and both relays enter in ON state. The middle module M_2 gets disengaged from the array through active contacts of relays, and its power is stored in the battery. The uppermost and lowest modules (M_1 and M_3) remain intact with the string as their respective opto-ICs are forward biased, while the bypass diode of the middle module provides the path for their common string current (I_{Sring}) as illustrated in Fig. 4(c).

In the proposed method, a curve scanning based MPPT is utilized. The principle operation of this method is to search the GM/MPP through tracing of the P-V curve via a separate parallel capacitor. The appropriate value of this capacitor can be designed to execute the fast scanning (in milliseconds) of the P-V curve [25]. Note that the proposed hardware scheme possesses the capability and flexibility to incorporate any other specialized MPPT for partial shading. Nevertheless, the aforementioned MPPT is selected because of its fast response and simple algorithm [25].

IV. SIMULATION RESULTS AND COMPARATIVE STUDY

In simulation experiments, two dynamic reconfiguration methods i.e., proposed method & Method [19] are modeled in the PSIM environment along with two configuration methods i.e., TCT & SP. The comparative analysis between these methods is conducted for the output power under the influence of three different partial shading conditions, which are shown in Fig. 5. A PV array of size 10×3 ($N_s \times N_p$) is used, where the specifications of each module are as follows: $V_{oc} = 10.78$ V, $I_{sc} = 3.45$ A, $V_{mpp} = 8.2$ V, $I_{mpp} = 3.22$ A, and $P_{mpp} = 26.4$ W. A boost converter is installed between PV array and battery load of 120 V. The designed values of converter's parameters are: $C_{in} = 100$ μF, $C_{out} = 150$ μF, and $L = 300$ μH.

Fig. 6 presents the two step processing of proposed method when PV array is subject to partial shading of Case-1. In *Step-*
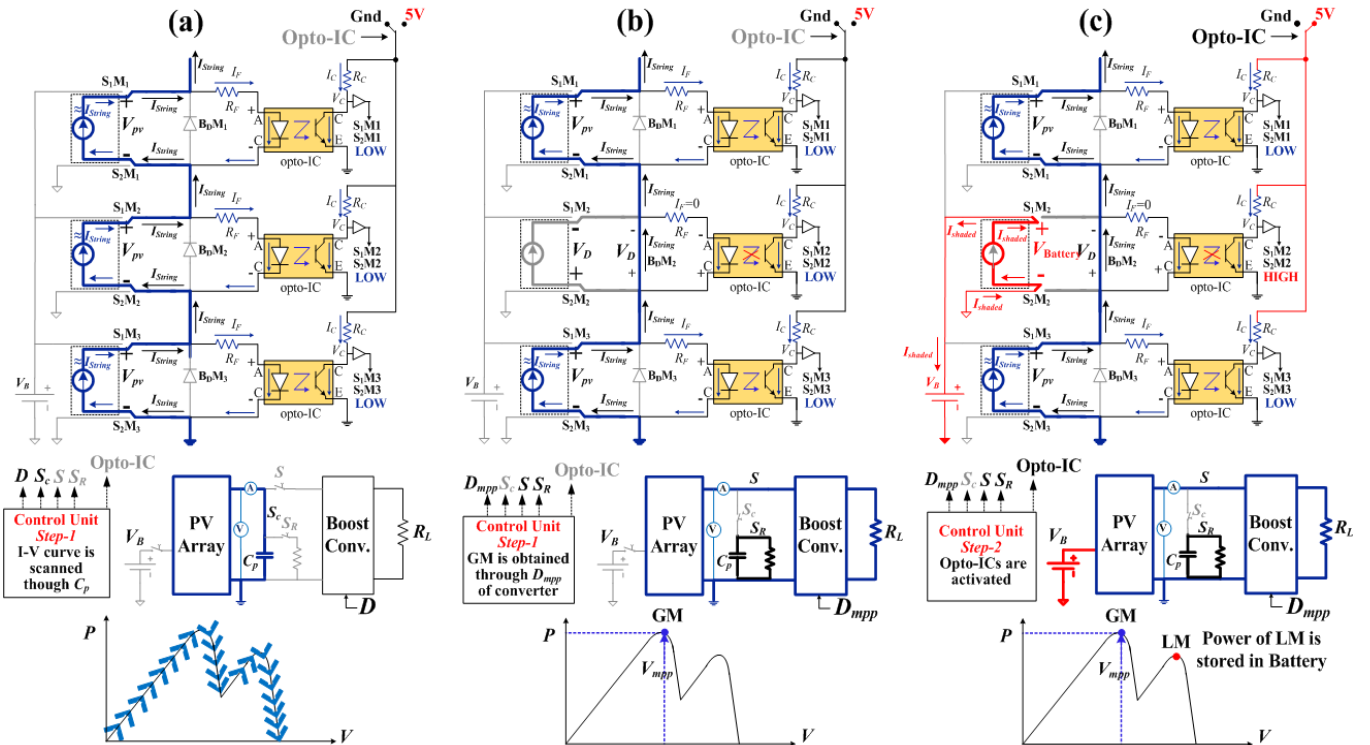

Fig. 4 Proposed hardware scheme under different operations: (a) PV organized in SP configuration and opto-ICs are disabled, (b) I-V curve is traced and GM is tracked through D-modulation of converter, (c) opto-ICs are enabled through which shaded module (M) is relocated to battery
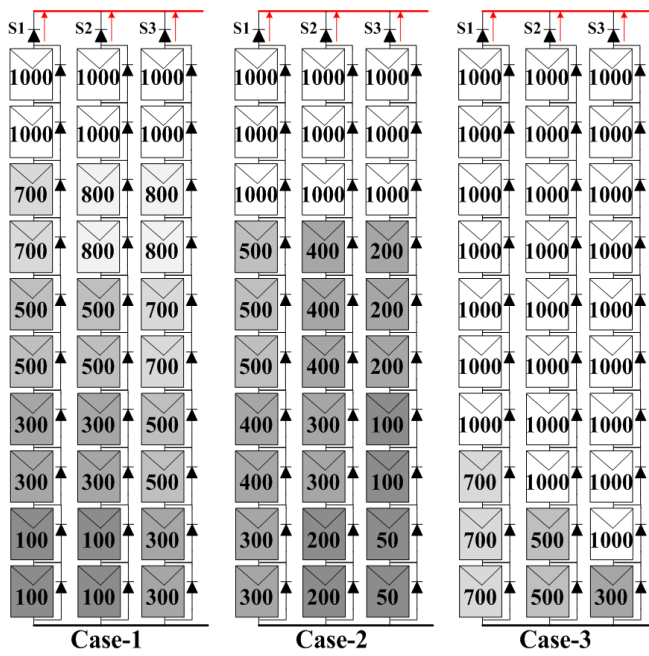
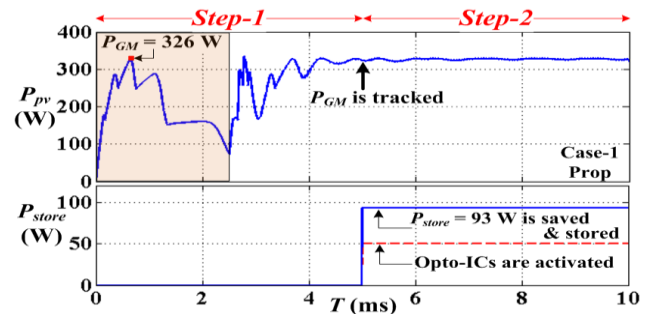Fig. 5 PV array of size 10x3 with three different shading patterns

Fig. 6 Control operation of proposed method under Case-1 shading pattern where net power of 419 W is extracted from array
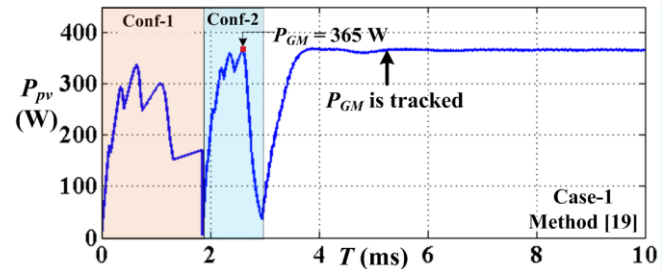

Fig. 7 Response of Method [19] under Case-1 shading pattern

1, all the opto-ICs are disabled and the P-V curve of an array arranged in SP configuration is traced to search the GM. The illustration of this step can be viewed in the highlighted portion of Fig. 6. Once, GM (= 326 W) is obtained at 5 ms through modulation of the duty cycle of boost converter, the control of the proposed method enters in *Step-2*. In this step, the biasing supply of opto-ICs is activated and bypass modules are identified with the help of their respective opto-ICs. Finally, these bypass modules are disengaged from PV array through relay switches and these modules are relocated in the parallel form with the battery of voltage rating of 8.25 V.

Under partial shading of Case-1, the bypass modules are capable of producing 93 W of power as shown in the lower graph of Fig. 6, which is stored in a battery. This simulation result indicates the 'one-click' storage of power by the proposed configuration. Importantly, it doesn't require any irradiance sensor, complex I-V models, searching and sorting algorithms, no physical movement of modules, and multiple tracings of P-V curve.

Fig. 7 shows the principle operation of Method [19] when partial shading of Case-1 is imposed on PV array. It configures the PV array into two different configurations. During each configuration, the control algorithm of Method [19] finds out the global maximum (GM), and whichever configuration exhibits the larger value of GM, Method [19] sets the PV array at that configuration. For instance, Method [19] configures the PV array in second configuration as it delivers the higher P_{GM}

of 365 W. It means that Method [19] scans the P-V curve twice for every new partial shading condition, and with that, managing the several peaks of the P-V curve of two different configurations bring complexity in the scheme.

The maximum power of the PV array against the present Case-1 when arranged in TCT and SP configurations are mentioned in Table 1. The report card of each configuration in terms of power yield is displayed in Table 1, where the percentage of extra power is calculated from the following formula:

$$\%P_{Advan} = \frac{P_{Prop} - P_{Conf}}{P_{Conf}} \times 100 \qquad (4)$$

where, P_{Prop} and P_{Conf} represent the power produced by proposed method and power generated by other configuration. Here, P_{Advan} indicates the percentage power advantage of the proposed method over others. It can be confirmed that in Case-1, the proposed method yields 14.8% more power than the Method [19]. At the same time, it yields 23.6% and 28.5% more power than TCT and SP configurations, respectively.

Under partial shading of Case-2 as shown in Fig. 5, the operation of proposed method is presented in Fig. 8, while the response of Method [19] is shown in Fig. 9. The power value of each method is mentioned in Table 1. It can be confirmed that proposed method delivers net power of 442 W, which

Table 1. Report card of each scheme in terms of power yield and %P_{Advan} of proposed scheme over others

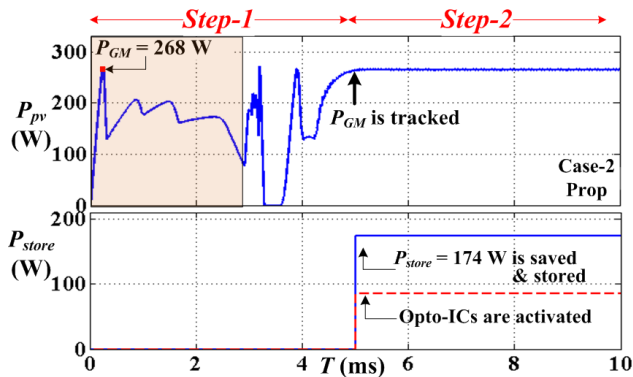| Cases	Net power extracted from PV array in watts (W)				%P_{Advan} of the Proposed method over other methods		
	Dynamic Reconfiguration Methods		Static Configuration Methods		Dynamic Reconfiguration Methods	Static Configuration Methods	
	Prop	Method [19]	TCT	SP	Method [19]	TCT	SP
1	419 W	365 W	339 W	326 W	14.8%	23.6%	28.5%
2	442 W	341 W	271 W	266 W	29.6%	63.1%	66.2%
3	784 W	690 W	700 W	683 W	13.6%	12.0%	14.8%

Fig. 8 Response of proposed method under Case-2 shading pattern where net power of 440 W is obtained from array
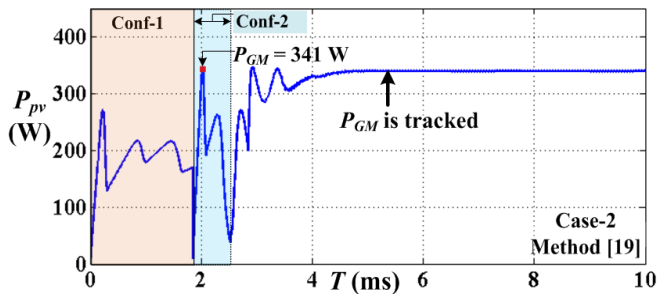

Fig. 9 Operation of Method [19] under Case-2 shading pattern

is 101 W more power than Method [19]. Simultaneously, the proposed method extracts additional power of 171 W and 176 W as compared to TCT (271 W) and SP (266 W) configurations, respectively.

In the final test i.e., Case-3 (Fig. 5), the performance of the proposed scheme is shown in Fig. 10, where it gathers 784 W of power from PV array. Once again, Method [19] lags behind the power yield of the proposed scheme by a significant margin as it delivers 690 W of power. The response of Method [19] is shown in Fig. 11. As far as TCT and SP are concerned, the proposed method still maintains a sizeable margin over these configurations in terms of power yield.

A bar plot is shown in Fig. 12, where the power bar of each method is normalized with respect to the proposed method as it always delivers superior power. The %power deficit of each method against each case is mentioned with regard to proposed method. Compared to the proposed scheme, the power deficit of other methods is highest under Case-2, while the power
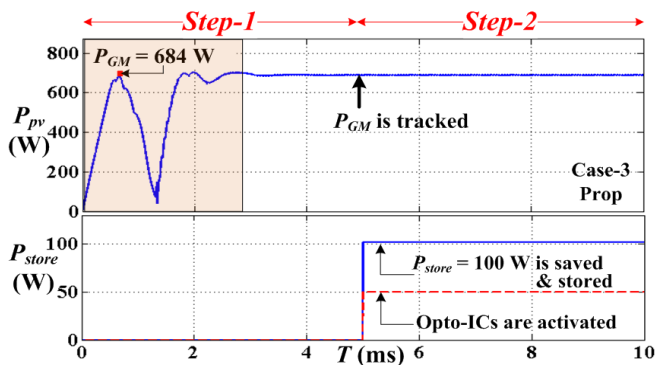

Fig. 10 Power saving and GM tracking of proposed method under Case-3 shading pattern
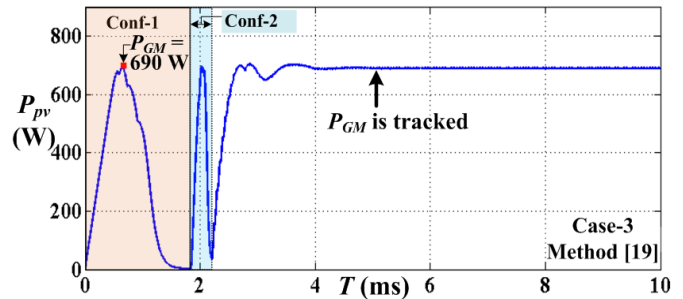

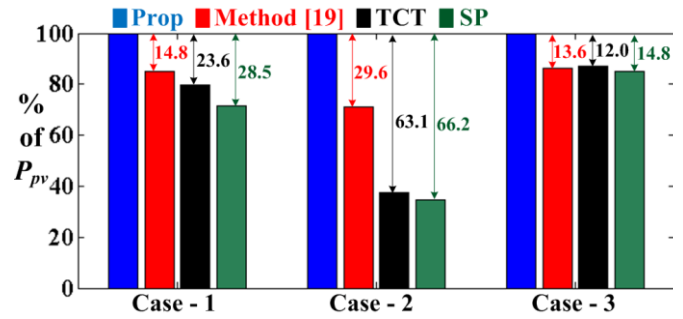Fig. 11 Power operation of Method [19] under Case-3

Fig. 12 Bar plot of schemes under three cases normalized with respect to proposed method

deficit becomes lowest during the shading condition of Case-3. During shading Case-1 and Case-2, Method [19] exhibits the second-best performance, while TCT shows better performance than Method [19] during Case-3.

V. EXPERIMENTAL VALIDATION AND RESULTS

An experimental prototype is developed for the validation of proposed scheme, which is shown in Fig. 13 along with labels. PV array is comprised of two modules, which are connected in series. The specifications of each module are mono-crystalline
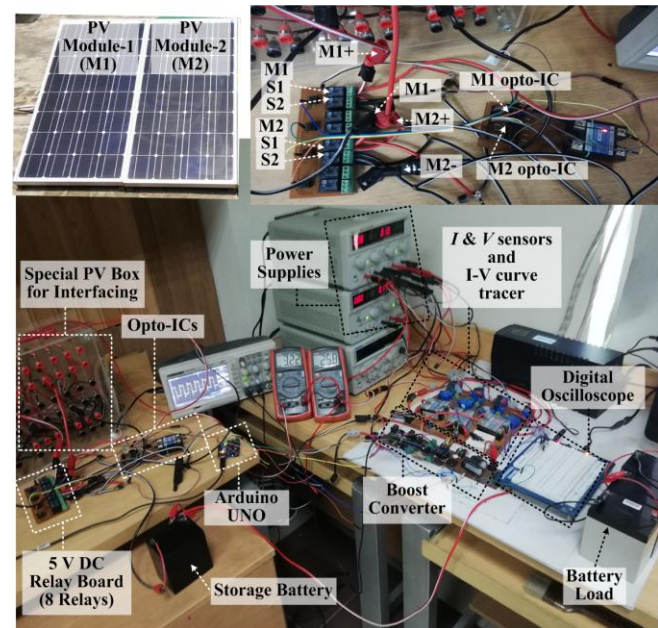

Fig. 13 Complete hardware prototype of proposed hardware scheme along with labels

technology - Model TSPM 85, V_{oc} = 19 V, V_{mpp} = 16.2 V, I_{sc} = 6 A, I_{mpp} = 5.25 A, and P_{mpp}= 85 W. Electromechanical relays of 5 V are used as switches S_1 and S_2 as presented in upper side of Fig. 13. The energy of bypass modules is stored in a separate battery of 12 V. PV array is interfaced with a battery load of 36 V through boost converter. The converter operates at a switching frequency of 40 kHz with the following values of components: C_{in} = 150 μF, C_{out} = 500 μF, and L = 330 μH.

To experimentally validate the concept of the proposed method, two distinct shading conditions are created arbitrarily on the PV array through opaque paper-card. Fig. 14 shows the response of the proposed method under the first shading condition, while Fig. 15 displays the system performance under the second shading condition. In both figures, four parameters of PV array are recorded through digital oscilloscope, which are: I_{pv} (blue-line), V_{pv} (red-line), P_{pv} (black-line), and P_{store} (pink-line). P_{Store} depicts the power of bypass modules, which is directed towards the storage battery.

For the first partial shading condition shown in Fig. 14, the system undergoes the routine two-step operation of proposed method as already outlined in Sec. III. In *Step-1*, the PV curve is scanned, while all the opto-ICs are disabled. Notice that PV array exhibits two LMs because of a particular shading pattern on it. Once GM of 39.33 W is obtained through the operation of boost converter, the proposed scheme enters in *Step-2*. In this *Step*, all opto-ICs are switched-on and bypass module is identified. Consequently, the power (11.28 W) of bypass module is stored in the battery as shown in P_{store} line in Fig. 14. Compared to SP configuration, the P_{Advan} is calculated from (4) as 28.7%. This value shows a good resemblance to the simulated data presented in Table 1.
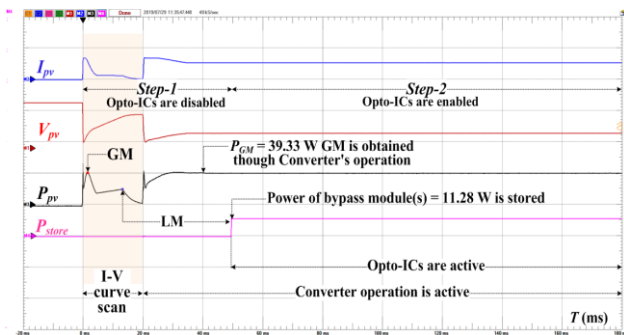

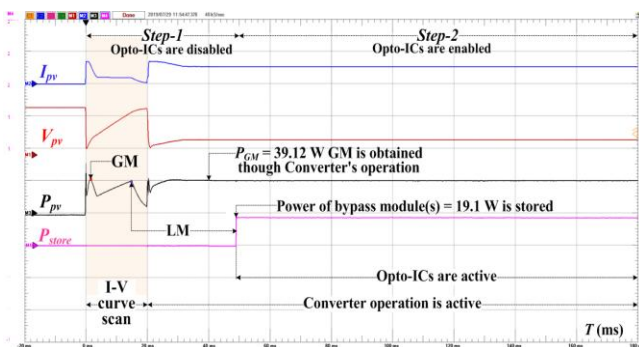Fig. 14 Practical response of the proposed method under first shading condition

Fig. 15 Practical response of the proposed method under mild second shading condition

For the second test, PV array is subject to mild shading condition compared to the previous case. Fig. 15 displays the result, where the P-V curve exhibits two closely matched LMs. In this scenario, when opto-ICs are triggered, the proposed scheme saves 19.1 W more power than a series-parallel configuration. This implies that the proposed scheme holds the significant power advantage of 48.8% over the series-parallel configuration. This practical result also highlights that nearly 50% power of bypass modules may be wasted under certain shading cases.

VI. Concluding Remarks

In this work, a new PV reconfigurable method based on module level electronic circuit is developed for the relocation of bypass PV modules, which works under partial shading conditions. The primary component of an electronic circuit is an optical device i.e., optocoupler. The scientific principle of the proposed method works in two simple steps:
1) In *Step-1*, all the modules are arranged in conventional series-parallel architecture, optical devices of modules are switched off and power-voltage (P-V) curve is traced to obtain the global maximum, and
2) In *Step-2*, the optical devices are made active, which detect the bypass modules and then relocate these modules through decentralized control to store their energy.

The identification and relocation of bypass modules are successfully executed by the proposed method through decentralized control of its module level electronic circuits. The proposed method displayed a significant advantage over other benchmark methods studied in the paper. In this manner, the proposed method contributes towards the progress of simplified power harvesting from the shaded PV array.

References

[1] T. S. Babu, J. P. Ram, T. Dragicevic, M. Miyatake, F. Blaabjerg, and N. Rajasekar, "Particle swarm optimization based solar PV array reconfiguration of the maximum power extraction under partial shading conditions flexible array switch matrix," *IEEE Transactions on Sustainable Energy*, vol. 9, no. 1, pp. 74–85, 2018.

[2] J. Storey, P. R. Wilson, and D. Bagnall, "The optimized-string dynamic photovoltaic array," *IEEE Transactions on Power Electronics*, vol. 29, no. 4, pp. 1768–1776, 2014.

[3] M. Akrami, and K. Pourhossein, "A novel reconfiguration procedure to extract maximum power from partially-shaded photovoltaic arrays," *Solar Energy*, vol. 173, pp. 110–119, 2018.

[4] R. Ahmad, A. F. Murtaza, H. A. Sher, H.A., U. T. Shami, and S. Olalekan, "An analytical approach to study partial shading effects on PV array supported by literature," *Renewable and Sustainable Energy Reviews*, vol. 74, pp. 721-732, 2017.

[5] O. Bingöl and B. Özkaya, "Analysis and comparison of different PV array configurations under partial shading conditions," *Solar Energy*, vol. 160, pp. 336–343, 2018.

[6] S. Malathy and R. Ramaprabha, "Reconfiguration strategies to extract maximum power from photovoltaic array under partially shaded conditions," *Renewable and Sustainable Energy Reviews*, vol. 18, part. 2, pp. 2922-2934, 2018.

[7] J. P. Storey, P. R. Wilson, and D. Bagnall, "Improved optimization strategy for irradiance equalization in dynamic photovoltaic arrays," *IEEE Transactions on Power Electronics*, vol. 28, no. 6, pp. 2946–2956, 2013.

[8] M. Dhimish, V. Holmes, B. Mehrdadi, M. Dales, B. Chong and L. Zhang, "Seven indicators variations for multiple PV array configurations under partial shading and faulty PV conditions," *Renewable Energy*, vol. 113, pp. 438-460, 2017.

[9] F. Iraji, E. Farjah, and T. Ghanbari, "Optimisation method to find the best

switch set topology for reconfiguration of photovoltaic panels," *IET Renewable Power Generation*, vol. 12, no. 3, pp. 374–379, 2018.

[10] Y. Mahmoud, and E. F. El-saadany, "Enhanced reconfiguration method for reducing mismatch losses in PV systems," *IEEE Journal of Photovoltaics*, vol. 7, no. 6, pp. 1746–1754, 2017.

[11] M. Matam and V. R. Barry, "Improved performance of dynamic photovoltaic array under repeating shade conditions," *Energy Conversion and Management*, vol. 168, pp. 639–650, 2018.

[12] M. L. Orozco-Gutierrez, G. Spagnuolo, J. M. Ramirez-Scarpetta, G. Petrone, and C. A. Ramos-Paja, "Optimized configuration of mismatched photovoltaic arrays," *IEEE Journal of Photovoltaics*, vol. 6, no. 5, pp. 1210–1220, 2016.

[13] S. Pareek, and R. Dahiya, "Enhanced power generation of partial shaded photovoltaic fields by forecasting the interconnection of modules," *Energy*, vol. 95, pp. 561–572, 2016.

[14] M. Jazayeri, K. Jazayeri, and S. Uysal, "Adaptive photovoltaic array reconfiguration based on real cloud patterns to mitigate effects of non-uniform spatial irradiance profiles," *Solar Energy*, vol. 155, pp. 506–516, 2017.

[15] G. Petrone, G. Spagnuolo, Y. Zhao, B. Lehman, C. A. R. Paja, and M. L. O. Gutierrez, "Control of photovoltaic arrays: Dynamical reconfiguration for fighting mismatched conditions and meeting load requests," *IEEE Industrial Electronics Magazine*, vol. 9, no. 1, pp. 62–76, 2015.

[16] A. S. Yadav, and V. Mukherjee, "Line losses reduction techniques in puzzled PV array configuration under different shading conditions," *Solar Energy*, vol. 171, pp. 774–783, 2018.

[17] M. Baka, P. Manganiello, D. Soudris, and F. Catthoo, "A cost-benefit analysis for reconfigurable PV modules under shading," *Solar Energy*, vol. 178, pp. 69-78, 2019.

[18] M. Manjunath, B. V. Reddy, and B. Lehman, "Performance improvement of dynamic PV array under partial shade conditions using M^2 algorithm," *IET Renewable Power Generation*, vol. 13, issue. (8), pp.1239-1249, 2019.

[19] A. A. Elserougi, M. S. Diab, A. M. Massoud, A. S. Abdel-Khalik, and S. Ahmed, "A switched PV approach for extracted maximum power enhancement of PV arrays during partial shading," *IEEE Transactions on Sustainable Energy*, vol. 6, issue. 3, pp.767-772, 2015.

[20] G. S. Krishna, and T. Moger, "Improved SuDoKu reconfiguration technique for total-cross-tied PV array to enhance maximum power under partial shading conditions," *Renewable and Sustainable Energy Reviews*, vol. 109, pp.333-348, 2019.

[21] V. M. R. Tatabhatla, A. Agarwal, and T. Kanumuri, "Improved power generation by dispersing the uniform and non-uniform partial shades in solar photovoltaic array," *Energy Conversion and Management*, vol. 197, 2019.

[22] N. Belhaouas, M-S. A. Cheikh, P. Agathoklis, M-R. Oularbi, B. Amrouche, K. Sedraoui, and N. Djilali, "PV array power output maximization under partial shading using new shifted PV array arrangements," *Applied Energy*, vol. 187, pp. 326–337, 2017.

[23] D. Li, G. Dong, L. Duan, D. Zhang, L. Wang, and Yong Qiu, "High-Performance organic optocouplers based on an organic photodiode with high blue light sensitivity," *IEEE Electron Device Letters*, vol. 34, no. 10, pp. 1295–1297, Oct. 2013.

[24] Accessed Online [2019] https://www.vishay.com/docs/83522/k817p.pdf.

[25] F. Spertino, J. Ahmad, A. Ciocia, P. Di Leo, A. F. Murtaza, and M. Chiaberge, "Capacitor charging method for I-V curve tracer and MPPT in photovoltaic systems," *Solar Energy*, vol. 119, pp. 461–473, 2015.

Ali Faisal Murtaza (M'16) received the B.Sc. degree from National University of Sciences and Technology (NUST), Rawalpindi, Pakistan, the M.Sc. degree from University of Engineering and Technology (UET), Lahore, Pakistan, and the Ph.D Degree from the Politecnico di Torino, Torino, Italy. He is currently working as Director Research and Assoociate Professor (Faculty of Engineering) in the University of Central Punjab (UCP), Lahore, Pakistan. At UCP, a research group "Efficient Electrical Energy Systems" is active under his supervision. His research interests include the design of Solar Photovoltaic (PV) systems including DC micro-grids, DC-DC converters, I-V Curve tracing, Maximum power point trackers, and partial shading effects. He is author/co-author of more than 35 publications.

Hadeed Ahmed Sher (S'14–M'17–SM'19) received the B.Sc. degree in Electrical Engineering from Bahauddin Zakariya University, Multan, Pakistan, in 2005, the M.Sc. degree in Electrical Engineering from the University of Engineering and Technology, Lahore, Pakistan, in 2008, and the Ph.D. degree in electrical engineering from King Saud University (KSU), Riyadh, Saudi Arabia, in 2016. He is currently an Assistant Professor with the Faculty of Electrical Engineering, Ghulam Ishaq Khan Institute of Engineering Sciences and Technology, Topi, Pakistan. His current research interests include grid connected solar photovoltaic systems, maximum power point tracking, and power electronics. He received the Research Excellence Award from the KSU College of Engineering for the year 2012 and 2015.

Kamal Al-Haddad (S'82-M'88-SM'92-F'07, LF'20) received the B.Sc.A. and M.Sc.A. degrees from the University of Québec à Trois-Rivières, Canada, in 1982 and 1984, respectively, and the Ph.D. degree from the Institute National Polythechnique, Toulouse, France, in 1988. Since June 1990, he has been a Professor with the Electrical Engineering Department, École de Technologie Supérieure (ETS), Montreal, QC, where he has been the holder of the senior Canada Research Chair in Electric Energy Conversion and Power Electronics since 2002. He has supervised more than 170 Ph.D. and M.Sc.A. students working in the field of power electronics. He is a Consultant and has established very solid link with many Canadian industries working in the field of power electronics, electric transportation, aeronautics, and telecommunications. He has coauthored more than 600 transactions and conference papers. His fields of interest are in high efficient static power converters, harmonics and reactive power control using hybrid filters, switch mode, resonant and multilevel converters including the modeling, control, and development of prototypes for various industrial applications in electric traction, renewable energy, power supplies for drives, telecommunication, etc. Prof. Al-Haddad is a fellow member of the Canadian Academy of Engineering. He is IEEE IES President 2016-2017, Associate editor of the Transactions on Industrial Informatics, IES Distinguished Lecturer and recipient of the 2014 IEEE IES Dr.-Ing. Eugene Mittelmann Achievement Award. Prof. Al-Haddad is a member of the Academy of Sciences and fellow of the Royal Society of Canada.

Filippo Spertino received his M. Sc and Ph.D. degrees in Electrical Engineering in 1995 and 2000, respectively, from Politecnico di Torino (PdT) university, Torino, Italy. Currently, he is an associate Professor (with full professor recognition within the Italian Scientific Qualification) in Electric Power Systems and Renewable Energy Systems with reference to Photovoltaic and Wind power systems at Energy Department, PdT. His research activities include design, simulation, experimental testing on Photovoltaic, Wind, storage power systems and instrument calibration. He was principal investigator of some research projects, regarding innovative photovoltaic applications with storage systems, funded by various companies. He participated to the following European Projects: PERSIL, SINGULAR, e-HIGHWAY 2050 and OSMOSE. He is senior member of: IEEE (since 2007 and 2018, respectively), Italian Association of Electrical, Electronic and Telecommunications Engineers (AEIT since 1994), CEI (Italian Electrotechnical Committee since 2007) and IEC, regarding Photovoltaic Energy Systems and Wind Energy Systems. He organized seminars, regarding PV and wind energy generation, at PdT on behalf of AEIT. He is author/coauthor of more than 100 publications: 40 on Journals, 2 chapters of books and the remainder on proceedings of Conferences.